Analysis of the Effect of Alloying Elements on the Martensite-start Temperature of the Steels

C. Capdevila, F. G. Caballero and C. García de Andrés*

Department of Physical Metallurgy, Centro Nacional de Investigaciones Metalúrgicas (CENIM) Consejo Superior de Investigaciones Científicas (CSIC), Avda. Gregorio del Amo, 8. 28040 Madrid, Spain. www.cenim.csic.es.

* Corresponding author. Tel.: 00-34-915538900; fax: 00-34-915347425

E-mail addresses: ccm@cenim.csic.es (C.Capdevila), fgc@cenim.csic.es (F.G. Caballero) and cgda@cenim.csic.es (C. García de Andrés)

Abstract

Making the transformation from austenite to martensite difficult is called *stabilisation of austenite,* a phenomenon that occurs in many cases. The straightforward method to analyse the influence of a specific factor on the stabilisation of austenite is through its influence on the martensite start (M_s) temperature. This work outlines the use of an artificial neural network to model the M_s temperature of engineering steels from their chemical composition and austenite grain size. The results are focussed on analysing the role in the stabilisation of austenite of alloying elements in steels including less common elements such as V and Nb, as well as the austenite grain size. Moreover, a physical interpretation of the results is presented.

1. Introduction

Microalloyed steels in the as-forged condition are commonly used in the automotive industry. For heavy-duty applications such as that for diesel engine crankshafts, a surface induction hardening heat treatment is carried out in critical regions of the components to enhance their service performance through adding strength and fatigue resistance. The goal of the induction hardening heat treatment is to form a fully martensitic structure in the outer surface of the component to locally increase the hardness and tensile strength. Thus, factors affecting martensitic transformation are of vital importance in the design of industrial processes of these engineering steels.

Making the transformation from austenite to martensite difficult is called *stabilisation of austenite,* which is due to a change in chemical composition, heat treatment or plastic deformation. [1] Of these three cases, chemical stabilisation is the most common; therefore, the influence of the chemical composition on the martensite start (M_s) temperature has been extensively reported in the literature for low alloy steels and several empirical equations have been proposed. [2-7] However, these empirical equations are not sufficiently general and are known to provide inaccurate answers for microalloyed steels, or steels whose compositional range are out of bounds from those used to formulate the equations.

On the other hand, Olson and Cohen [8] developed a model for heterogeneous martensitic nucleation that obviates the need for pre-existing embryos with martensitic structure, but requires a suitable nucleating defect in austenite. The initial defect might be a group of dislocations in an austenite-austenite interface [9] or frozen-in vacancies obtained by quenching form austenitisation temperature. [10] Therefore, grain boundaries and other lattice imperfections may also act as nucleation sites and contribute to make the

austenite phase unstable. On the contrary, they can also contribute to the stabilisation of the austenite phase by hindering the growth of the transformation product. [10] Which of these various contributions predominates depends on the chemical composition and the nature of the imperfections.

It is followed that to find out how the austenite grain size and alloying elements, including those used as microalloying elements (V and Nb), can affect the M_s temperature is an important issue to be investigated. The aim of this work is to develop an artificial neural network model to predict the M_s temperature of steels and interpret the influence of the chemical composition and the austenite grain size. Neural networks are useful whenever the intricacy of the problem is overwhelming from a fundamental perspective and where simplification is unacceptable. They represent a powerful method of non-linear regression modelling.

2. The experimental database

The definition of the M_s temperature in any model ideally requires a complete description of the chemical composition and the austenite grain size. A search of the literature [9-15] allow us to collect 320 individual cases where detailed chemical composition, prior austenite grain size (PAGS), and M_s values were reported.

Table l shows the list of 15 input variables used for the M_s temperature analysis. It was possible to find 270 cases where all of these variables were reported with the exception of nitrogen concentrations. It would have been unreasonable to set this latter concentration to zero when its value is not reported. Steels inevitably contain this impurity element in practice. For cases where the N value was missing its concentration was set to the mean value calculated for the 320 cases of the database. For the other

elements such as Mn, Ni, etc, the concentrations can truly be set to zero when they are not reported. This is because they would not be deliberate added or would have concentrations close to the limits of chemical analysis with the techniques generally used [16].

3. Brief description of neural network

The aim is to be able to estimate the M_s temperature as a function of the variables listed in Table 1. The analysis was carried out using variables normalised between +0.5 and –0.5; this normalisation is not necessary for the analysis, but allows a convenient comparison of the influence of individual input variables on an output. The normalisation procedure is expressed quantitatively as

$$x_N = \frac{x - x_{min}}{x_{max} - x_{min}} - 0.5 \qquad (1)$$

where x_N is the normalised value of x which has maximum and minimum values given by x_{max} and x_{min} respectively.

The network consisted of 15 input nodes (Table 1), a number of hidden nodes, and an output node representing the M_s temperature (Fig. 1). The network was trained using a randomly chosen of 170 examples from a total of 320 available; the remaining 150 examples were used as new experiments to test the trained network.

Linear functions of the inputs x_j are operated by a hyperbolic tangent transfer function

$$h_i = \tanh\left(\sum_j w_{ij}^{(1)} x_j + \theta_i^{(1)} \right) \qquad (4)$$

so that each input contributes to every hidden unit. The bias is designated θ_i and is analogous to the constant that appears in linear regression. The strength of the transfer

function is in each case determined by the weight w_{ij}. The transfer to the output y is linear

$$y = \sum_i w_i^{(2)} h_i + \theta^{(2)} \quad (3)$$

This specification of the network structure, together with the set of weights, is a complete description of the formula relating the inputs to the output. The weights were determined by training the network and the details are described by MacKay [17-18]. The training involves a minimisation of the regularised sum of squared errors. The term σ_v used below was the framework estimation of the noise level of the data. The complexity of the model was controlled by the number of hidden units (Fig. 2).

Figure 2 shows that the inferred noise level decreases monotonically as the number of hidden units increases. However, the complexity of the model also increases with the number of hidden units. A high degree of complexity may not be justified, and in an extreme case, the model may in a meaningless way attempt to fit the noise in the experimental data. MacKay [19-20] has made a detailed study of this problem and defined a quantity (the 'evidence') which comments on the probability of a model. In circumstances where two models give similar results for the known data, the more probable model would be predicted to be that which is simpler; this simple model would have a higher value of evidence. The evidence framework was used to control σ_v. The number of hidden units was set by examining performance on test data. A combination of Bayesian and pragmatic statistical techniques were therefore used to control the complexity of the model. [19-21]

Figure 3 shows that a large number of hidden units did not give significantly lower values of σ_v; indeed, the test set error has a minimum at three hidden units. Therefore, three hidden units were found to give a reasonable level of complexity to represent the variations of M_s temperature as a function of the input variables of Table 1. The levels

of agreement for the training and test data are shown in Fig. 4(a) and 4(b); good predictions occur in both instances.

4. Use of the model

4.1 Effect of microalloying elements

The main advantage of the neural network model as compared with other empirical models is the ability of analysing separately the influence on the stabilisation of austenite of each one of the alloying elements. In this sense, the role of microalloying elements such as V and Nb on M_s temperature has been analysed in this section.

Figure 5 shows the influence of V and Nb on M_s temperature for three different grades of carbon and considering a constant *PAGS* of 20 μm. It is clear from this figure that the higher microalloying content, the higher M_s temperature. This effect is more pronounced as carbon concentration increases. It is possible to get a physical understanding of these results. According to their chemical properties, V and Nb can be classified as very strong carbide formers. This behaviour may be attributed to the influence of alloying elements on the activity of carbon in the solid solution. Keeping this in mind, we can expect that interactions between carbon and carbide former elements tend to weaken the role of carbon rising thus M_s. Likewise, these interactions are stronger as carbon content increases.

This is consistent with the following thermodynamic considerations. In the thermodynamic approach presented by Bhadeshia [22-23], martensitic transformation is said to be triggered when the chemical driving force ($\Delta G^{\gamma\alpha'}$) achieves a critical value at the M_s temperature ($\Delta G_C^{\gamma\alpha'}$). Following Olson and Cohen, [24] Ghosh and Olson [9]

proposed that the total energy describing the heterogeneous semicoherent nucleation process of martensite is given by the sum of a defect dislocation energy and a fault energy. At sufficient driving force (obtained by cooling or an applied stress), the fault energy becomes negative and gives rise to a barrierless condition where a nucleus can grow spontaneously, at a rate controlled by the interfacial mobility. The critical condition for semicoherent nucleation is then given by a balance between the negative fault energy and the interfacial frictional work. Therefore, Gosh and Olson proposed that $\Delta G_C^{\gamma\alpha'}$ is the addition of two terms. The former includes the fault energy, and the latter is the interfacial frictional work between the austenite matrix and martensite nucleus which is composition dependent. The critical value in J mol^{-1} of the driving force needed to trigger martensitic transformation is:

$$\begin{aligned} -\Delta G_C^{\gamma\alpha'} = {} & 1010 + 4009c_C^{0.5} + 1879c_{Si}^{0.5} + 1980c_{Mn}^{0.5} + 172c_C^{0.5} + 1418c_{Mo}^{0.5} + 1868c_{Cr}^{0.5} \\ & + 1618c_V^{0.5} + 752c_{Cu}^{0.5} + 714c_W^{0.5} + 1653c_{Nb}^{0.5} + 3097c_N^{0.5} - 352c_{Co}^{0.5} \end{aligned} \quad (7)$$

where $c^{0.5}$ are the square root of the alloying elements concentration in mole fraction. The coefficients were obtained by Ghosh and Olson by establishing the $c^{0.5}$ dependence and fitting over a wide range of compositions: the maximum concentrations were approximately 2 wt.-% for carbon and nitrogen, 0.9 wt.-% vanadium and about 2-28 wt.-% for all the other alloying elements. [25]

The thermodynamic calculations involved here have been performed using the commercial software package, MTDATA. [26] The two sublattice model [27] was used to express the Gibbs free energies of ferrite and austenite phases. The first sublattice is occupied by substitutional atoms and the second is occupied by interstitial atoms and vacancies. The Gibbs free energies of austenite, G^{γ}, and ferrite of the same composition,

G^{α}, were calculated separately by allowing only one phase to exist in the system. Then, the molar Gibbs free energy differences, $\Delta G^{\gamma\alpha} = G^{\alpha} - G^{\gamma}$, at different temperatures were obtained. The Gibbs free energies of both phases include unitary terms of free energies, mixing entropies, excess free energies describing the deviation from the regular solution model, and magnetic contributions. However, to calculate $\Delta G^{\gamma\alpha'}$ also requires an estimation of the Zener ordering energy, [28] which arise because carbon atoms in ferrite can in some circumstances order on one of available sublattices of octahedral interstitial sites, thereby changing the symmetry of the lattice from bcc to bct. The ordering temperature, T_c, is a function of the carbon concentration [29]. If the M_s temperature exceeds T_c then the martensite is bcc, but when it is below T_c martensite is bct. The ordering energy is a complicated function of temperature and carbon concentration, and was calculated as in Ref. 29. The required free energy is then given by $\Delta G^{\gamma\alpha'} = \Delta G^{\gamma\alpha} + G_{Zener}$.

Figures 6 and 7 show the evolution of $\Delta G^{\gamma\alpha'}$ for different grades of V and Nb for carbon concentration of carbon C=0.1 wt.-% and C=0.8 wt.-%. It is suggested from these figures that the influence of the microalloying elements on M_s temperature is small for the lower value of carbon concentration (C=0.1 wt.-%) meanwhile the higher carbon content (C=0.8 wt.-%), the more influence on rising M_s temperature.

4.2 Effect of grain size on the stabilisation of austenite

Figure 8 shows the influence of *PAGS* on M_s temperature in a Fe-C steel. It is clear from this figure that an increase on M_s is achieved if the *PAGS* increases. Likewise, Fig. 8 shows that the lower carbon content, the higher increase in M_s temperature.

As it was mentioned in the previous section, the temperature of initiation of martensitic transformation, and its progress are controlled by the chemical and non-chemical free energies of the system. The chemical free energy difference ($\Delta G^{\gamma\alpha'}$) is the driving force of the transformation and is converted to non-chemical free energy. The latter partly goes into the energy of lattice imperfections inevitable upon transformation. [10]

In carbon steels, the morphology of martensite changes with the carbon content. The martensite consists of bundles of laths (lath-shaped martensite) with a high density of dislocations inside each lath in low carbon steels and, as carbon content increases, it changes to lenticular (lens-shaped martensite) with a midrib and a high density of dislocations as well as internal twins. [30]

Several studies [31-34] have documented a clear effect of *PAGS* on M_s temperature in ferrous systems. Unemoto and Owen [31] carried out a definitive study of the effect of grain size in bursting-type Fe-Ni-C alloys. These authors concluded that the M_s temperature in these alloys is influenced by the PAGS because of the interference with the autocatalytic nature of the burst-type martensitic transformation. However, they describe the martensite morphology as lath-shaped martensite, and lath martensite transformation is often associated with grain boundaries. [32] A nucleation argument, therefore, would suggest higher M_s temperature (*i.e.* easier nucleation) as grain size is decreased since grain boundary area increases. In the present analysis, the opposite effect is observed.

On the other hand, Brofman and Ansell [33] proposed that the Hall-Petch strengthening of the austenite explains the depression of M_s temperature as PAGS decreases. Hirth [35] has reviewed various theories of grain size strengthening in metals and reported some experimental evidence for the expression

$$\rho \propto \frac{1}{D} \tag{8}$$

where ρ is the dislocation density and D is the austenite grain diameter. If this argument is valid, Hall-Petch strengthening results from increasing dislocation density with decreasing grain size, thus directly strengthening the matrix, *i.e.* the austenite. Therefore, a reduction of the grain size will increase the resistance of the austenite to plastic deformation locally as well as macroscopically. This increased austenite resistance will directly impede the martensite transformation by increasing the non-chemical free energy opposing the transformation. [36] This theory explains the drop in M_s temperature as *PAGS* decreases. However fails to explain why M_s temperature increases faster as *PAGS* increases in low carbon (C=0.1 wt.-%) than in a high carbon (C=0.8 wt.-%) steels.

An alternative explanation is outlined considering that higher austenitisation temperatures are required to achieve the same *PAGS* in low carbon steels than in high carbon steels. Therefore, a more likely cause of rising the M_s temperature as *PAGS* increases is the reduction of the energy needed for the complementary shear during transformation, which originates in the elimination of lattice imperfections due to higher austenitisation temperature. [37] Likewise, the nucleation of martensite may be boosted by an increase of frozen-in vacancies into the austenite grain due to higher quenching temperatures in low carbon steels. The increase in vacancies makes the austenite phase less stable by increasing the nucleation sites [9,37]. Therefore, assuming the austenitisation temperature and the quenching temperature identical, M_s temperature should increase as austenitisation temperature increases since a higher quenching temperature produces more frozen-in vacancies and hence more nucleation sites.

4.3 Validation of the model

Figure 9 shows a comparison between the neural network model predictions and the experimentally measured M_s temperatures carried out in five very different alloys whose actual compositions are listed in Table 2. S1 and S2 are low carbon HSLA steels microalloyed with Nb, S3 and S4 are medium carbon forging steel with and without Nb as microalloying element, respectively, and S5 is a commercial martensitic stainless steel. All of these are used for commercial purposes, and therefore, their M_s temperature is a critical parameter whose determination is important in the processing route of the steel. Hence, its accurate determination is very interesting from an industrial point of view. It could be concluded from the figure that the neural network model presents an excellent accuracy on M_s temperature prediction.

5. Conclusions

A neural network method based on a Bayesian framework has been used to rationalise an enormous quantity of published experimental data on M_s temperature of steels. It is now possible, therefore, to estimate the role of elements such as V and Nb whose use as microalloying elements has recently increased due to the good combination of mechanical properties that microalloyed steels present.

The formulated neural network model has been also applied towards the understanding of the role of the austenite grain size on stabilising the austenite or, by contrast, on triggering the martensite transformation. The increase of M_s temperature as *PAGS* increases seems to reveal that the reduction of lattice imperfections and the increase in frozen-in vacancies due to higher austenitisation temperatures increases martensite nucleation sites and then enhance the transformation. It has been demonstrated that the

model gives a good estimation of the experimental M_s temperatures obtained in different kinds of commercial steels.

6. Acknowledgements

The authors acknowledge financial support from Comisión Interministerial de Ciencia y Tecnología (PETRI 1995-0436-OP). F.G. Caballero would like to thank the Consejería de Educación, D.G. de Investigación de la Comunidad Autónoma de Madrid (CAM) for the financial support in the form of a Postdoctoral Research Grant. C. Capdevila would like to express his gratitude to the Consejo Superior de Investigaciones Cientifícas for financial support as a Post-Doctoral contract (I3P PC-2001-1). The authors gratefully acknowledge to Prof. H.K.D.H. Bhadeshia F.R.S of the University of Cambridge for his fruitful discussions.

7. References

1. J.W. Christian: ‘Theory of phase transformations in metals and alloys’, 803; 1965, Oxford, Pergamon press.
2. L.A. Capella: *Metal. Prog*., 1944, **46**, 108-118.
3. J. Wang, P.J. van der Wolk and S. Van der Zwaag: *Mater. Trans. JIM*, 2000, **41**, 761-768.
4. R.A. Grange and HM. Stewart: *Trans. AIME*, 1946, **167**, 467-494.
5. P. Payson and H. Savage: *Trans ASM*, 1944, **33**, 261-280.
6. C.Y. Kung and J.J. Rayment: ‘Hardenability Concepts with Applications to Steels’, 229; 1978, Warrendale, PA, TMS-AIME.
7. K.W. Andrews: *JISI*, 1965, **203**, 721-727.
8. G.B. Olson and M. Cohen: *Metall. Trans. A*, 1976, **7A**, 1897-1923.
9. G. Ghosh and G.B. Olson: *Acta Metall. Mater*., 1994, **42**, 3361-3370.
10. Z. Nishiyama: ‘Martensitic Transformation’, (ed.: M. E. Fine *et al*.), 13; 1978, New York, Academic Press.
11. M. Economopoulos, N. Lambert, and L. Habraken: ‘Diagrames de transformation des aciers fabriques dans le Benelux’, 80; 1967, Bruxelles, Centre National de Reserches Metakllurgiques.
12. M. Atkins: ‘Atlas of continuous cooling transformation diagrams for engineering steels’, 17; 1985, Sheffield, British Steels Corporation.
13. J. Wang, P. Van der Wolk and S. Van der Zwaag: *ISIJ Int*., 1999, **39**, 1038-1046.
14. F.G. Caballero, H.K.D.H. Bhadeshia, K.J.A. Mawella, D.G. Jones and P. Brown: *Mater. Sci. Technol*., 2001, **17**, 517-522.

15. F.G. Caballero, H.K.D.H. Bhadeshia, K.J.A. Mawella, D.G. Jones and P. Brown: *Mater. Sci. Technol*., 2001, **17**, 512-516.
16. T. Cool, H.K.D.H. Bhadeshia and D.J.C. MacKay: *Mat. Sci. Engineer*., 1997, **A233**, 186-200.
17. D.J.C. MaKay: *Neural Comput*., 1992, **4**, 698-705.
18. D.J.C. MaKay: *Darwin college J*., 1993, 81-93.
19. D.J.C. MaKay: *Neural Comput*., 1992, **4**, 415-422.
20. D.J.C. MaKay: *Neural Comput*., 1992, **4**, 448-460.
21. H.K.D.H. Bhadeshia: *ISIJ Int*., 1999, **39**, 965-979.
22. H.K.D.H. Bhadeshia: *Met. Sci*., 1981, **15**, 175-177.
23. H.K.D.H. Bhadeshia: *Met. Sci*., 1981, **15**, 178-180.
24. G.B. Olson and M. Cohen: *Metall. Trans. A*, 1976, **7A**, 1905-1914.
25. G.B.Olson and M. Cohen: *Metall. Trans.*, **7A**, 1976, 1915-1923.
26. Metallurgical and Thermochemical Databank, 1996, Teddington, Middlessex, National Physical Laboratory.
27. M. Hillert and L.I. Staffansson: *Acta Chem. Scand*., 1970, **24**, 3618-3625.
28. C. Zener: *Trans. AIME*, 1946, **167**, 513-550.
29. J.C. Fisher: *Trans. AIME*, 1949, **185**, 688-690.
30. Z. Nishiyama: 'Martensitic Transformation', (ed.: M. E. Fine *et al*.), 28; 1978, New York, Academic Press.
31. M. Unemoto and W.S. Owen: *Metall. Trans.*, 1975, **5**, 2041-2053.
32. O.A. Ankara, A.S. Sastri, and D.R.F. West: *J. Iron and Steel Institute*, 1966, **May**, 509-511.
33. P.J. Brofman and G.S. Ansell: *Metall. Trans. A*, 1983, **14A**, 1929-1931.
34. T. Maki, S. Shimooka, and I. Tamura: *Metall. Trans*., 1971, **2**, 2944-2955.

35. J.P. Hirth: *Metall. Trans*., 1972, **3**, 3047-3065.

36. E.M. Breinan and G.S. Ansell: *Metall. Trans*., 1970, **1**, 1513-1520.

37. Z. Nishiyama, 'Martensitic Transformation', (ed.: M. E. Fine *et al*.), 307; 1978, New York, Academic Press.

Table 1. Variables that influence Ms temperature. SD is standard deviation

	Range	Average	SD
C, wt.-%	0 – 1.62	0.3774	0.2098
Mn, wt.-%	0 – 1.98	0.8652	0.4882
Si, wt.-%	0 - 3.400	0.2328	0.3836
Cr, wt.-%	0 - 17.98	1.4255	3.2575
Ni, wt.-%	0 - 27.20	1.9705	5.3646
Mo, wt.-%	0 - 5.10	0.1850	0.4611
V, wt.-%	0 - 4.55	0.0758	0.3579
Co, wt.-%	0 - 12.27	0.0820	0.8145
Al, wt.-%	0 - 1.10	0.0187	0.1183
W, wt.-%	0 - 12.99	0.1269	1.0665
Cu, wt.-%	0 - 0.28	0.0388	0.0778
Nb, wt.-%	0 - 0.2	0.0004	0.0048
B, wt.-%	0 - 0.001	0.0000	0.0001
N, wt.-%	0.0001-0.0140	0.0015	0.0039
PAGS, μm	5 - 339	55.1731	37.3855

Table 2. Chemical compositions and *PAGS* of the steel tested.

	% C	% Mn	% Si	% Cr	% Ni	% Mo	% V	% Nb	PAGS, μm
S1	0,07	1,50	0,37	0,039	0,49	0,021	0,004	0,027	9
S2	0,20	1,10	0,34	0,011	0,02	0,008	0,009	0,003	10
S3	0,31	1,22	0,25	0,138	0,09	0,03	0,004	0	21
S4	0,60	0,49	0,35	14,52	0,17	0,57	0,18	0	50
S5	0,37	0,34	0,94	4,80	0	1,34	1,19	0	30

Figure 1.- Neural Network model used in this study

Figure 2. Variation of σ_V as a function of hidden units.

Figure 3. Variation of test error as a number of hidden units.

Figure 4. Comparison between predicted and experimental Ms values: (a) training data and (b) test data.

Figure 5. Effect of (a) V and (b) Nb on Ms temperature. PAGS=20 μm.

Figure 6. Effect of V on $\Delta G^{\gamma\alpha'}$ and $\Delta G_C^{\gamma\alpha'}$ for (a) C=0.1 wt.-% and (b) C=0.8wt.-%. Horizontal lines represent $\Delta G_C^{\gamma\alpha'}$.

Figure 7. Effect of Nb on $\Delta G^{\gamma\alpha'}$ and $\Delta G_C^{\gamma\alpha'}$ for (a) C=0.1 wt.-% and (b) C=0.8wt.-%. Horizontal lines represent $\Delta G_C^{\gamma\alpha'}$.

Figure 8. Effect of *PAGS* on Ms temperature for a Fe-C steel.

Figure 9. Comparisson between experimental and calculated Ms temperature for the steels listed in Table 2.

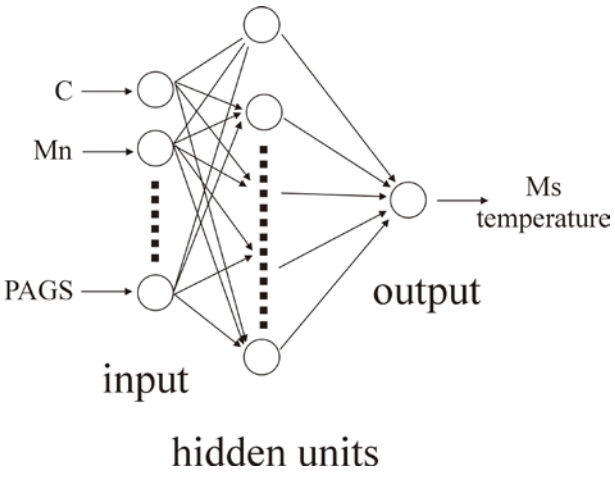

Figure 1.- Neural Network model used in this study

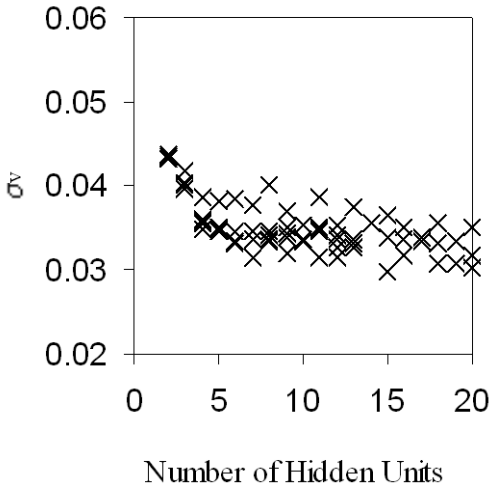

Figure 2. Variation of σ_V as a function of hidden units.

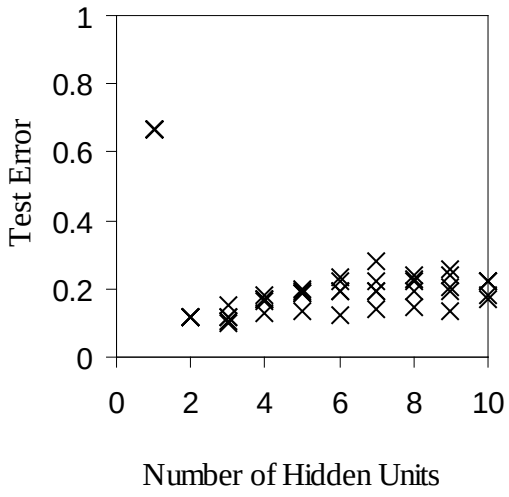

Figure 3. Variation of test error as a number of hidden units.

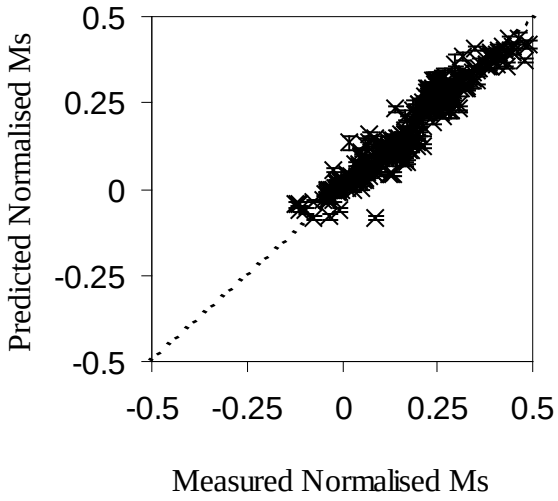

(a)

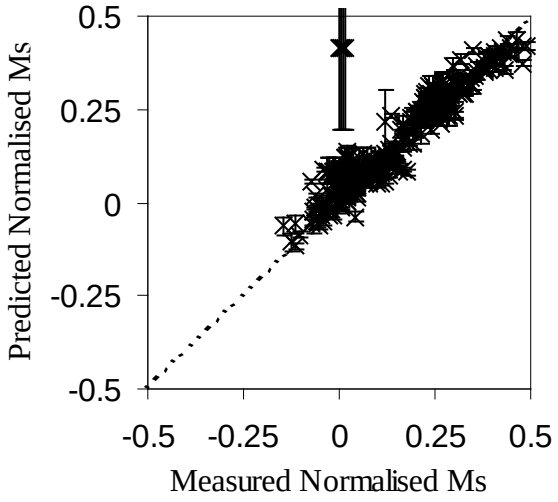

(b)

Figure 4. Comparison between predicted and experimental Ms values: (a) training data and (b) test data.

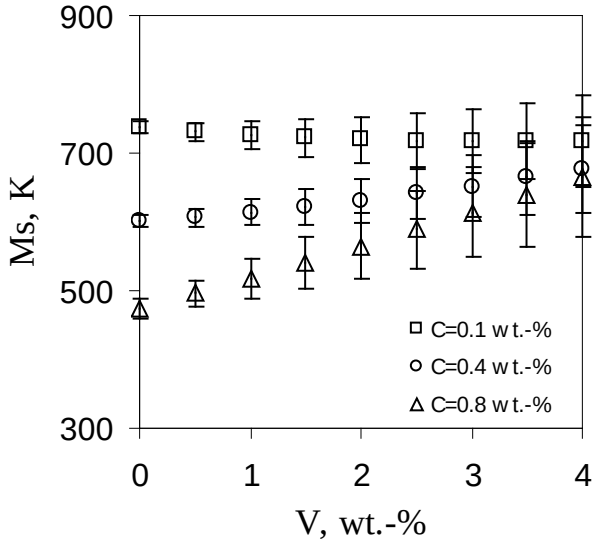

(a)

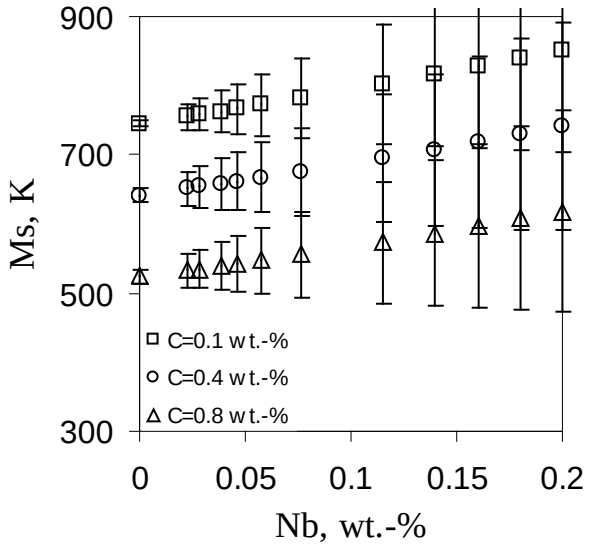

(b)

Figure 5. Effect of (a) V and (b) Nb on Ms temperature. PAGS=20 μm.

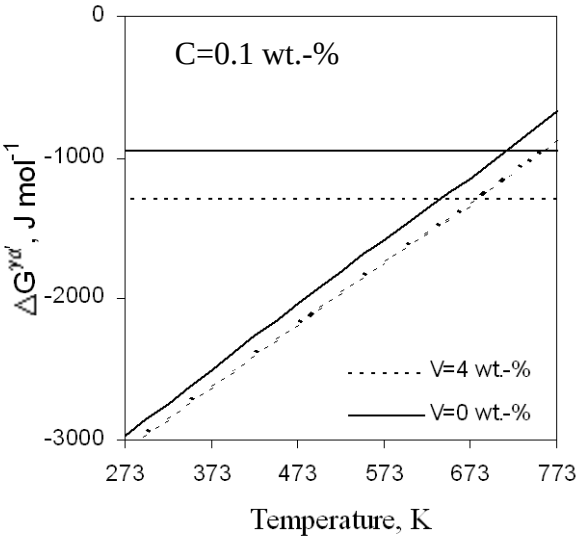

(a)

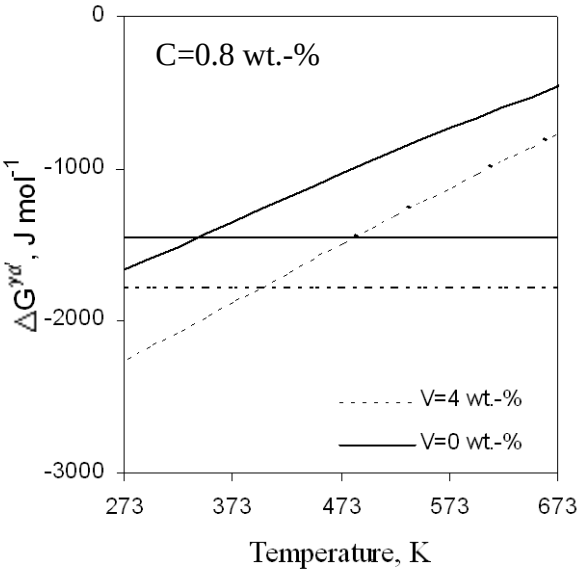

(b)

Figure 6. Effect of V on $\Delta G^{\gamma\alpha'}$ and $\Delta G_C^{\gamma\alpha'}$ for (a) C=0.1 wt.-% and (b) C=0.8wt.-%.

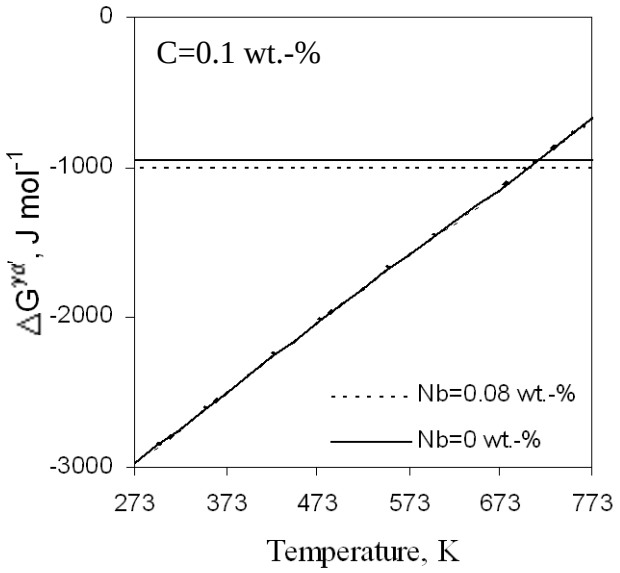

(a)

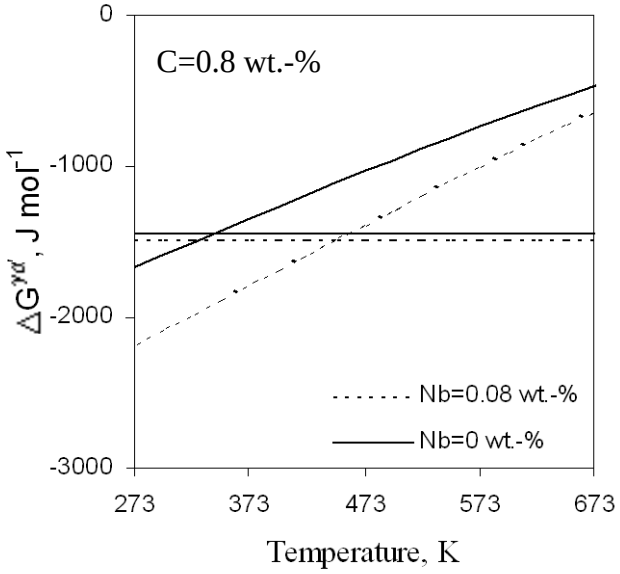

(b)

Figure 7. Effect of Nb on $\Delta G^{\gamma\alpha'}$ and $\Delta G_C^{\gamma\alpha'}$ for (a) C=0.1 wt.-% and (b) C=0.8wt.-%.

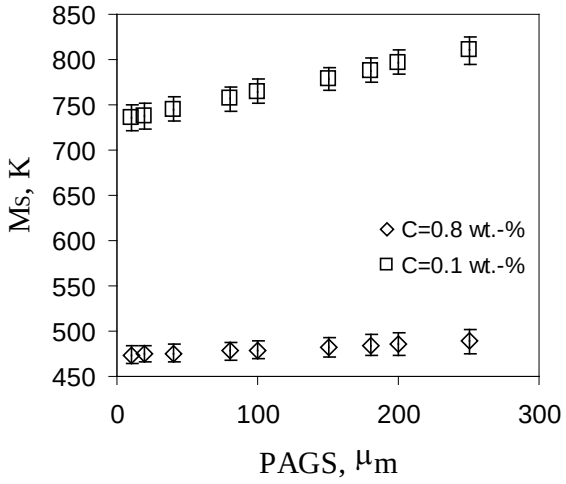

Figure 8. Effect of *PAGS* on Ms temperature for a Fe-C steel.

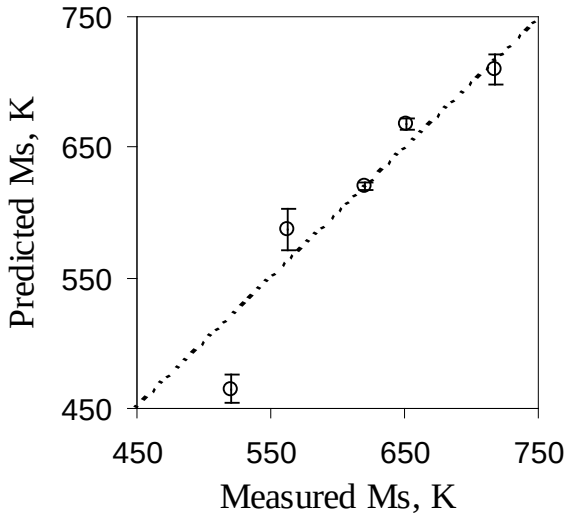

Figure 9. Comparisson between experimental and calculated Ms temperature for the steels listed in Table 2.